Ground Robot Navigation Relies on Blimp Vision Information

Rami Al-Jarrah and Hubert Roth

***Abstract*—Blimp and ground robots have received much attention in the research due to their strong potential in the explorations tasks. There are many applications where a robot must explore an area without previous knowledge of the environment. This work presents a system composed by a blimp and ground robots that cooperates and share visual information to address those requirements. To realize this task, an efficient vision-based object detection and localization algorithm is proposed by using Speeded up Robust Features technique. A navigation system for ground robot was proposed supported by vision data from the blimp robot. These data are optimized by fuzzy sets model to correct the prediction position information of the ground robot and the obstacles in its pathway. Based on these data, a navigation and obstacle avoidance system is used to control the ground vehicle trajectory. The overall system has been tested in actual missions, and results show that the system has good results in navigation and it is effective, robust and suitable for complex tasks.**

***Index Terms*—Blimp robot, ground robot, fuzzy logic, computer vision.**

I. Introduction

Recently, unmanned aerial vehicle have been used extensively in exploration, surveying and reconnaissance applications. A combined between the aerial and ground robots have been studied and developed because such system can provide aerial imagery and perception along with ground robot inspection capabilities. It can be used for several purposes in civil and military applications. Some of those applications are focused on using ground robots to help in dangerous tasks, as well as to explore large unstructured environments. Hence, a robot must be able to navigate from an initial to a target point without colliding with other vehicles or obstacles. This navigation can be described as the problem of finding a suitable and collision-free motion of the ground robot, while obstacle mapping consists of using the sensing capabilities to obtain the representation of unknown obstacles in such a manner that it is useful for navigation [1]. Blimp and ground robots have the peculiarity to be endowed with different characteristics. By merging all those capacities and characteristics together, it is possible to develop a unique sensing and perception collaborative system. In other words, as a typical lighter-than-air vehicle, the autonomous blimp robot is a unique and promising platform for many different kinds of applications, such as telecommunication, broadcasting relays, disaster guard, and scientific exploration [2]. The blimp robot not only creates a good opportunity to explore the environments, but also it increases the efficiency of the exploration since it has many advantages over the small airplanes robots such as long time hovering, much less energy consumed, very low noise and cost efficiency which made them ideal for exploration of areas without disturbing environment [3]. On the other hand, visual navigation, especially for humans and vehicles, is currently one of the most active research topics in computer vision. Actually, the increasing in the applications of robots has made the computer vision an important factor in such research area not only to put cameras in place of human eyes, but it is also to accomplish the entire task as autonomous as possible. Computer vision is demonstrated being a powerful as well as a non-intrusive and low cost sensor useful for many applications in robotics and control system. Hence, many robots can carry a light camera and use the images obtained by cameras in autonomous tasks. Perhaps the most common way to classify the computer vision in robots depends on the complexity degree of the applications. The common process in vision system is called a visual tracking that is analyzing of sequential images to identify a reference pattern and follow a moving interest point or defined object over time on the image. There are many tracking methods in which the algorithms based on features, color and shape [4]. The visual odometry analyzed images to extrapolate the robot space movement relies on the image motion, then to estimate the position and orientation of the robot [5]. The next process is the visual navigation which uses the visual data to determine object position as well as the safe path [6]. The visual navigation can be classified as map-based system. In this way, the robot makes a self-localization in which the images are matched to known map in order to update robot position. Concerning to visual navigation, several reactive and deliberative navigation approaches have been proposed such as in structured environments using white line recognition [7], in corridor navigation using View-Sequenced Route Representation [8], or more complex techniques combining visual localization with the extraction of valid planar region [9], or visual and navigation techniques to perform visual navigation and obstacle avoidance [10]. The aerial-ground robots have the peculiarity to be endowed with different characteristics. By merging all those characteristics together, it could be possible to develop a unique sensing and perception collaborative system. In [11], they study a multi-robot system depends on a vision-guide autonomy quad-rotor and describe a methods to take off, land and track over the ground robot. However, the quad-rotor does not provide information to the ground robot about the surrounding environment. Also, [12] presents a motion-planning and control system based on visual servoing

Manuscript received November 3, 2013; revised January 22, 2014.

The authors are with the Control and Automatic Engineering Department, Siegen University, Germany (e-mail: {rami.al-jarrah, Hubert.roth}@uni-siegen.de).

DOI: 10.7763/IJCCE.2014.V3.294

without cameras on board. In [13], they integrated and fuse vision data from the aerial and ground robots for best target tracking and for allowing leveraging of multi-domain sensing and increase opportunities for improving line of sight communications. These studies and others have been tested for several purposes such as environment monitoring [14], fire detection and fighting [15] and multi purposes collaborative tasks [16].

In this paper a strategy that takes advantage of mixed robotic system heterogeneity for collaborative navigation and obstacle avoidance is addressed. In other words, the ground robot navigation is supported by visual information from the blimp robot. The advantage of using an aerial visual navigation system is that the robot can do a pseudo-zoom on an obstacle and the possibility to identify other unexpected navigation obstructions in the environment. This collaboration ensures the ground robot safety while it performs other inspection missions without require a previous knowledge of this environment.

The free collision navigation system is being developed in several phases. First step, the ground robot and any obstacles in the pathway are recognized, detected and localized by using the blimp images based on Speeded up Robust Features technique SURF. This algorithm is real-time vision-based object detection which is running on the real-time operating system LINUX. Then, the vision information is optimized by using fuzzy sets model and possibilities histograms. Therefore, some techniques are applied to enable simple navigation and obstacle avoidance.

This paper is organized as follows. First, the problems regarding geometric projections, Aerial- Ground robot navigation are stated. Section III presents the vision-based robot localization. Then, we introduce the fuzzy sets model system in Section IV. Finally, the first results obtained and the conclusions are presented.

II. The Problem Definition

In this section the projections and coordinate system which are important to use the image obtained with the camera mounted on the blimp's gondola in order to detect the ground robot and the obstacles in the environment. The goal is to obtain the relative distance between the ground robot and any obstacle in the area. The coordinate frame system is illustrated in Fig. 1. In this work, we have used the image acquisition process which knows as the pinhole camera model that defines the geometric relationship between a 3D point and its 2D corresponding projection onto the image plane. By using a pinhole camera model, this geometric mapping from 3D to 2D is called a perspective projection [17]. There are two types of parameters need to be recovered to reconstruct model. The parameters that define the location and orientation of the camera reference frame with respect to the world frame which they called extrinsic camera parameters. Then, the intrinsic parameters which link the pixel coordinate of the image point with corresponding coordinate in the camera reference frame.

The ideal pinhole camera model describes the relationship between a 3D point $(X, Y, Z)^T$ and its corresponding 2D projection (u, v) onto the image plane as it is illustrated in Fig. 1. The projection of a 3D world point $(X, Y, Z)^T$ onto the image plane at pixel position $(u, v)^T$ can be written as:

$$x = -\left(x_{pf} - o_x\right) \times s_x \tag{1}$$

$$y = -\left(y_{pf} - o_y\right) \times s_y \tag{2}$$

where (o_x, o_y) are the coordinate of the principal point, s_x, s_y correspond to the effective size of the size of the pixels.

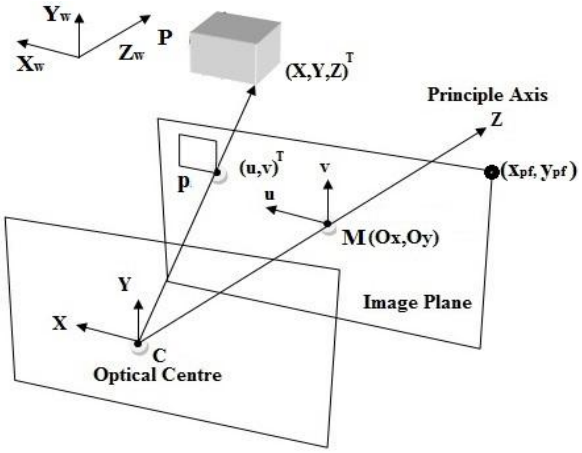

Fig. 1. The perspective projection model.

The coordinate of the most right-top points is (x_{pf}, y_{pf}). By using the matrix notation:

$$\begin{bmatrix} x_{pf} \\ y_{pf} \\ 1 \end{bmatrix} = \begin{bmatrix} -1/s_x & 0 & o_x \\ 0 & -1/s_y & o_y \\ 0 & 0 & 1 \end{bmatrix} \begin{bmatrix} x \\ y \\ 1 \end{bmatrix} \tag{3}$$

The matrix that contains the intrinsic camera parameters is given by:

$$M_{in} = \begin{bmatrix} -f/s_x & 0 & o_x \\ 0 & -f/s_y & o_y \\ 0 & 0 & 1 \end{bmatrix} \tag{4}$$

where f is the focal length. The matrix which contains the extrinsic camera parameters is given by:

$$M_{ex} = \begin{bmatrix} r_{11} & r_{12} & r_{13} & -R_1^T T \\ r_{21} & r_{22} & r_{23} & -R_2^T T \\ r_{31} & r_{32} & r_{33} & -R_3^T T \end{bmatrix} \tag{5}$$

where R and T are the parameters that identify uniquely the rotation matrix and translation vector between the unknown camera reference frame and the known world reference frame, respectively.

$$R = \begin{bmatrix} r_{11} & r_{12} & r_{13} \\ r_{21} & r_{22} & r_{23} \\ r_{31} & r_{32} & r_{33} \end{bmatrix} \tag{6}$$

By implementing and using homogeneous coordinates between (4) and (5), the projection matrix can be given as:

$$\begin{bmatrix} x_h \\ y_h \\ w \end{bmatrix} = M_{in} M_{ex} \begin{bmatrix} X_w \\ Y_w \\ Z_w \\ 1 \end{bmatrix} = M \begin{bmatrix} X_w \\ Y_w \\ Z_w \\ 1 \end{bmatrix} \quad (7)$$

$$= \begin{bmatrix} m_{11} & m_{12} & m_{13} & m_{14} \\ m_{21} & m_{22} & m_{23} & m_{24} \\ m_{31} & m_{32} & m_{33} & m_{34} \end{bmatrix} \begin{bmatrix} X_w \\ Y_w \\ Z_w \\ 1 \end{bmatrix}$$

where M is the combining the extrinsic with intrinsic camera parameters matrices and it is called the projection matrix. Therefore, the relation of 3D points and their 2D projections can be seen as a linear transformation from the projective space $(X_w, Y_w, Z_w, 1)^T$ to the projective plane $(x_h, y_h, w)^T$. Then, the pixel coordinates by using homogenization are given by (8) and (9).

$$x_{pf} = \frac{x_h}{w} = \frac{m_{11}X_w + m_{12}Y_w + m_{13}Z_w + m_{14}}{m_{31}X_w + m_{32}Y_w + m_{33}Z_w + m34} \quad (8)$$

$$y_{pf} = \frac{y_h}{w} = \frac{m_{21}X_w + m_{22}Y_w + m_{23}Z_w + m_{24}}{m_{31}X_w + m_{32}Y_w + m_{33}Z_w + m34} \quad (9)$$

In order to find the perspective camera model, assuming $o_x = o_y = 0$ and $s_x = s_y = 1$ then:

$$M_p = \begin{bmatrix} -fr_{11} & -fr_{12} & -fr_{13} & fR_1^T T \\ -fr_{21} & -fr_{22} & -fr_{23} & fR_2^T T \\ r_{31} & r_{32} & r_{33} & -R_3^T T \end{bmatrix} \quad (10)$$

To verify the correctness of the above matrix:

$$M_p P_w = \begin{bmatrix} -fR_1^T & fR_1^T T \\ -fR_2^T & fR_2^T T \\ R_3^T & -R_3^T T \end{bmatrix} \begin{bmatrix} P_w \\ 1 \end{bmatrix} = \begin{bmatrix} -fR_1^T (P_w - T) \\ -fR_2^T (P_w - T) \\ R_3^T (P_w - T) \end{bmatrix} \quad (11)$$

After homogenization we get:

$$u = -f \frac{R_1^T (P_w - T)}{R_3^T (P_w - T)} = f \frac{X_c}{Z_c} \quad (12)$$

$$v = -f \frac{R_2^T (P_w - T)}{R_3^T (P_w - T)} = f \frac{Y_c}{Z_c} \quad (13)$$

where f is the focal length.

III. Vision System

We have designed an embedded system and software architecture for the blimp robot as well as proposed a computer vision algorithm to realize a blimp robot follow ground robot and keep it within the camera view in our previous work [18], [19]. Based on these works, we update the algorithm in order to detect the ground robot and the obstacle in the environment (multi detection objects). After many experiments and since the execution time depends on the size of the image (Window), it was found that the size 168x264 pixels is the best choice because it is fast and more accurate.

A visual system has been used in order to localize the ground robot and the obstacle in the environment by considering these criteria: performance, repeatability, accuracy and speed. In other words, we seek a detection method which allows having good detection with scaled invariant, rotation invariant, and robust against noise. The captured images from the camera are processed in order to localize the ground robot and Obstacle inside the image. Then, the correspondence between the location on the image and the location on work field has been made. The examination of the different approaches for object detection shows that Speeded up Robust Feature technique (SURF) is the most convenient for our demands. Our chosen was based on that particularly because SURF is fast and could be run effectively on the embedded on-board system.

The SURF algorithm has three main steps [20]. First, the selection of interest points which characterize distinctive regions in the image. Then, building feature vector for each interest point based on the neighboring pixels (window). The interest points and the feature vectors are computed for both the reference image and the captured image. Finally, a matching operation is conducted to retrieve the corresponding interest points on both images. The algorithm compares the distance between the feature vectors for reference image and those for the captured image. The SURF descriptor is a 64 element vector that calculated in a domain oriented with the assigned angle and sized according to the scale of the feature. The descriptor is estimated using horizontal and vertical response histograms calculated in a 4×4 grid. The first variant provides a 32 element vector and another vector provides 128 element vectors. The set of matched points between two images are frequently used to calculate geometrical transformation models and homographies. However, these sets points usually suffered from two kinds of errors. First, the measurements of the point position that follows the Gaussian distribution. Second, the outliers those describe the mismatched points given by the selected algorithm and Gaussian error distribution. Thus, in order to filter the total set of matched points to detect and eliminate the error, the Random Sample Consensus RANSAC algorithm has been used [21].

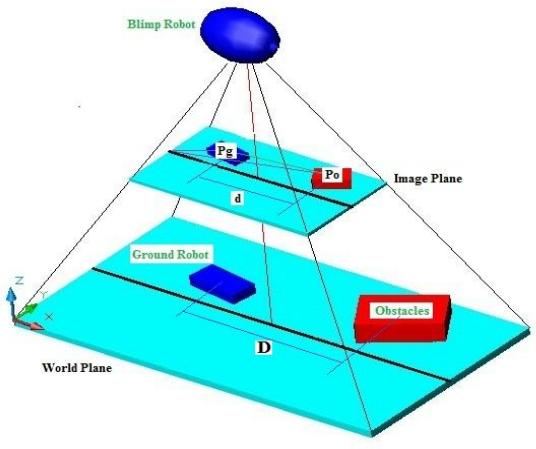

Fig. 2. Coordinate frame of the system.

Let us define $I(x, y)$ is the image frame. The coordinates of the most left-bottom and the most right-top points are (0, 0) and (263,167), respectively. The pose (location and orientation) of the ground robot is $P_g = (x_g, y_g, \theta_g)$ and the obstacle pose is $P_o = (x_o, y_o, \theta_o)$ in the image plane. These locations and orientations are related to camera projection point in the image plane and it is not global localization as shown in Fig. 2.

$$\theta_g = \tan^{-1}\left(\frac{x_g}{y_g}\right) \quad (14)$$

$$\theta_o = \tan^{-1}\left(\frac{x_o}{y_o}\right) \quad (15)$$

$$d_g = \sqrt{x_g^{\,2} + y_g^{\,2}} \quad (16)$$

$$d_o = \sqrt{x_o^{\,2} + y_o^{\,2}} \quad (17)$$

$$d_g^o = \sqrt{(x_o - x_g)^2 + (y_o - y_g)^2} \quad (18)$$

$$\theta_g^o = \tan^{-1}\left(\frac{x_o - x_g}{y_o - y_g}\right) \quad (19)$$

where d_g and d_o (in pixels) are the distance of the ground robot centre projection point and distance of obstacle projection point with respect to the blimp projection point. θ_g and θ_o are the angle between the projection of the ground robot and blimp's path projection and the angle between the obstacle projection point and blimp's path projection. d_g^o and θ_g^o are the position and orientation of the ground robot related to the obstacle in image frame as shown in Fig. 3.

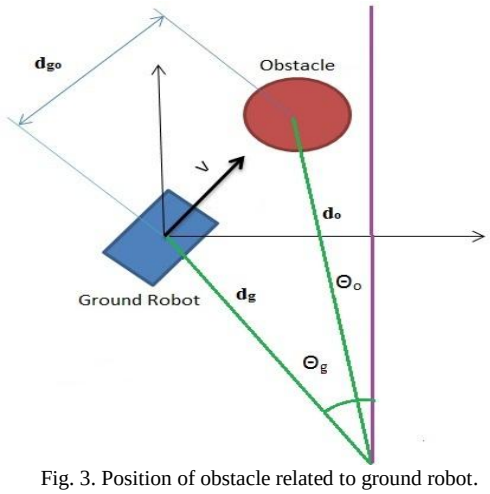

Fig. 3. Position of obstacle related to ground robot.

The metric distance D between the ground robot and the obstacle is obtained by using (13) as the following:

$$D = -\frac{H_b \times d_g^o}{f} \quad (20)$$

where H_b is the blimp altitude.

IV. Fuzzy Sets Model

In order to correct the prediction distance information between the ground robot and the obstacle that is gained from the SURF algorithm, a fuzzy sets model was needed. The classical fuzzy semantics are interpretations of fuzzy sets which represent cognitive categories and the system measurements are based on "linguistic variables". The main problem in the fuzzy control is how to design the fuzzy knowledge base. Thus, the combination between the possibility theory and fuzzy sets leads to model the complex systems empirically without regard to the presence of the human agent or expert [22]. Therefore, many experiments were done to study the effect of the distance between the ground robot and the obstacle. The general measuring data were collected for different distances (d_{go}), then we analyzed these data to propose fuzzy sets model by using possibilities histograms. The distance takes range (20,180) in pixels. A summary of these experiments and the errors are given in Table I. Based on the frequency distributions of these data, we could categorize them into four main groups as it is summarized in Table II. Then, we analyzed these groups in order to find the vectors ($\vec{A}$) and random set values (S). The mathematics of the random sets are complicated, but in the finite case which means they take values on subsets of universal Ω they could be seen simply as the following:

$$S = \{< A_i, \delta_i >: \delta_i > 0\} \quad (21)$$

where: A is the measuring record subset, δ_i is the evidence function.

TABLE I: The D-Error Analysis

d(Pixels)	Error	Vector	Sets
[160-180]	[-4,6]	<-4,6>	{[-4,6]}
[140-160]	[-4,4]	<-4,4>	{[-4,4]}
[120-140]	[-3,2]	<-3,2>	{[-3,2]}
[100-120]	[-3,2]	<-3,2>	{[-3,2]}
[80-100]	[-2,1]	<-2,1>	{[-2,1]}
[60-80]	[-2,1]	<-2,1>	{[-2,1]}
[40-60]	[-4,3]	<-4,3>	{[-4,3]}
[20-40]	[-5,4]	<-5,4>	{[-5,4]}

TABLE II: The Frequency Distributions Categories

Data	A_i	S_i
[140-180]	<[-4,4], [-4,6]>	{[-4,4]=0.5, [-4,6]=0.5}
[100-140]	<[-3,2], [-3,2]>	{[-3,2]=0.5, [-3,2]=0.5}
[60-100]	<[-2,1], [-2,1]>	{[-2,1]=0.5, [-2,1]=0.5}
[20-60]	<[-5,4], [-4,3]>	{[-5,4]=0.5, [-4,3]=0.5}

TABLE III: The Frequency Distributions Categories

Ei^L	E_i^R	$C_i(\Omega)$	$Supp_i(\Omega)$
{-4,-4}	{4,6}	{-4, 4}	{(-4,4), (4,6)}
{-3,-3}	{2,2}	{-3,2}	{(-3,2)}
{-2,-2}	{1,1}	{-2,1 }	{(-2,1)}
{-5,-4}	{4,3}	{-4,-4}	{(-5,-4),(-4,4), (4,3)}

The form of possibility histogram and distributions (π) depends on the core and support of the measurement record sets as it is shown in Table III. The core and support of the possibilities distribution for the histogram is given by:

$$C_i(\pi) = \left[E_i^L, E_i^R\right] \quad (22)$$

$$Sup_i(\pi) = \left[E_i^L, E_i^R\right] \quad (23)$$

where E_i^L and E_i^R are the left and right endpoints vectors, respectively. The possibilities histograms for the data as shown in Fig. 4 can be transferred to fuzzy membership functions without any changes due to fact that both of them has the same mathematical description and all possibilistic histogram are fuzzy intervals.

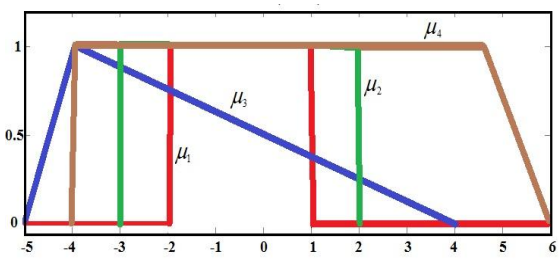

Fig. 4. Fuzzy Membership functions.

This fuzzy sets model could calculate the four membership functions, and then can correct the vision information as in (24).

$$\mu_d(i) = Sup\{\mu(\xi, r)\}, 1 < i < 4 \quad (24)$$

In order to estimate the distance d, the t-norms should be used as in (25)

$$Supp(\mu) = \sum_{i=1}^{4} d_\mu \quad (25)$$

V. Experimental Results

In order to verify the complete proposed system, some experiments were conducted. During these experiments the blimp robot was flying at a certain altitude (1 meter). These algorithms produced good result as shown in Fig. 5 and Fig. 6. The experiment was done in lab, the background is very clear and there is not any disturbance except for the illumination variance. We assume that the ground robot is already in the view of the on-board camera. The ground robot and the obstacle would be identified and detected in the video sequence by the vision system. One obstacle was taken into account during these experiments. The related distances and orientations between the ground robot and the obstacle are shown in in Fig. 7 and Fig. 8. These initial tests were implemented to check the feasibility of the system and the results are quite good and show how the ground robot can navigate by using the visual information.

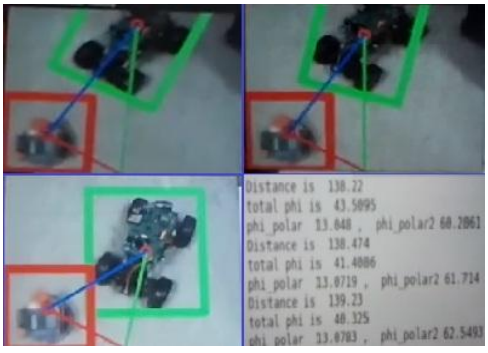

Fig. 5. SURF algorithm tests

Fig. 6. Experiments images sequences.

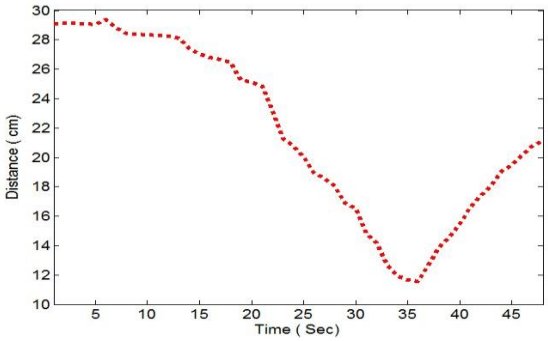

Fig. 7. The related distance d_{go}.

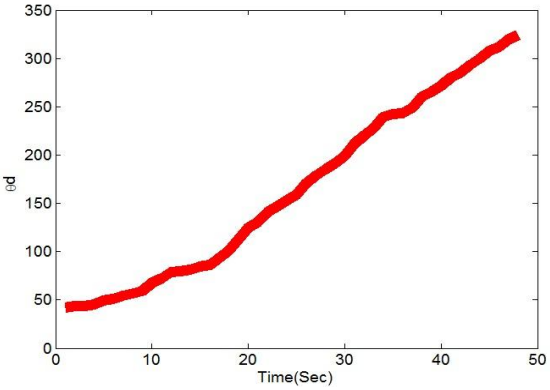

Fig. 8. The related oriented angle.

VI. Conclusion

In this paper, we have proposed an efficient vision-based object detection and localization algorithm to realize the autonomous ground navigation schema using images from a blimp robot. The prediction visual information is optimized by fuzzy sets model. In addition, the transformations from different coordinate frames have been formulated. The experiments results validate that the algorithm is not only able to help the ground robot navigates effectively, but also it improves the robustness and accuracy of the system. However, this algorithm could face some limitations in case the flying robot moves with high horizontal speed. In addition, the vision sensor characteristics could affect the performance. In the future, more extensive tests and more complex control are needed to create more complex architecture which allows in next phases to build local-maps and obtain a position of the

obstacles seen by the blimp as well as find the optimal path for the ground robot by using genetic algorithm. Also, these obstacles will be memorized and a global map with all obstacles will be built to enable the system to merge reactive and deliberative methods.

REFERENCES

[1] H. Choset, K. Lynch, S. Hutchinson, G. Kantor, W. Burgard, L. Kavraki, and S. Thrun, *Principles of Robot Motion: Theory, Algorithms, and Implementations*, Boston, MA: MIT Press, 2005.

[2] A. Chu and M. Blackmore, "Novel concept for stratospheric communications and surveillance: star light," in *Proc. AIAA Balloon System Conf.*, 2007, pp. 1-9.

[3] T. Xu and Y. Lu, "Onboard controlling system design of unmanned airship," in *Proc. International Conference on Electronic & Mechanical Engineering and Information Technology*, 2011, vol. 6, pp. 3028- 3031.

[4] M. Mikolajczyk and C. Smid, "A performance evaluation of local descriptors," *IEEE Trans. Pattern Analysis and Machine Intelligence*, vol. 27, no. 10, pp. 1615-1630, 2005.

[5] D. Nister, O. Naroditsky, and J. Bergen, "Visual odometry for ground vehicle applications," *Journal of Field Robotics*, vol. 23, no. 1, pp. 3-20, 2006.

[6] F. Bonin-Font, A. Ortiz, and G. Oliver, "Visual navigation for mobile robots: A survey," *Journal of Intelligent and Robotic Systems*, vol. 53, pp. 263-296, 2008.

[7] S. Ishikawa, H. Kuwamoto, and S. Ozawa," Visual navigation of an autonomous vehicle using white line recognition. pattern analysis and machine intelligence," *IEEE Transactions on*, vol. 10, no. 5, pp. 743 –749, September 1988.

[8] Y. Matsumoto, M. Inaba, and H. Inoue, "Visual navigation using view sequenced route representation," in *Proc. IEEE International Conference on In Robotics and Automation*, April 1996, vol. 1, pp. 83 –88.

[9] N. X. Dao, B. J. You, and S. R. Oh, "Visual navigation for indoor mobile robots using a single camera," in *Proc. IEEE/RSJ International Conference on Intelligent Robots and Systems*, August, 2005, pp. 1992–1997.

[10] A. Cherubini and F. Chaumette, "Visual navigation with obstacle avoidance," in *Proc. IEEE/RSJ International Conference on Intelligent Robots and Systems*, September 2011, pp. 1593 –1598.

[11] W. Li, T. Zhang, and K. A Klihnlenz, "Vision-guided autonomous quadrotor in an air-ground multi-robot system," *In Proc. 2011 IEEE International Conference on Robotics and Automation (ICRA)*, Shanghai, China, May 2011, pp. 2980-2985.

[12] R. Rao, V. Kumar, and C. Taylor, "Visual servoing of a UGV from a UAV using differential flatness," *In Proc. IEEE/RSJ International Conference on Intelligent Robots and Systems (IROS)*, Las Vegas, NV, USA, 2003, pp. 743–748.

[13] M. Moseley, B. P. Grocholsky, C. Cheung., and S. Singh, "Integrated long-range UAV/UGV collaborative target tracking," in *Proc. SPIE, Unmanned Systems Technology XI Conference*, 2009.

[14] A. Elfes, M. Bergerman, J. H. Carvalho, E. C. Paiva, J. J. Ramos, and S. S Bueno, "Air-ground robotic ensembles for cooperative applications: Concepts and preliminary results," in *Proc. 2nd International Conference on Field and Service Robotics*, Pittsburgh, PA, USA, 1999, pp. 75–80.

[15] C. Phan and H. Liu," A cooperative UAV/UGV platform for wildfire detection and fighting," in *Proc. Asia Simulation Conference: 7th International Conference on System Simulation and Scientific Computing*, Beijing, China, 2008, pp. 494–498.

[16] J. Valente, A. Barrientos, A. Martinez, and C. Fiederling, "Field tests with an aerial–ground convoy system for collaborative tasks," in *Proc. 8th Workshop de RoboCity2030-II*, Madrid, Spain, 2010, pp. 233–248.

[17] R. Hartley and A. Zisserman, *Multiple View Geometry in Computer Vision*," 2nd ed., Cambridge University Press, U.K, 2003, pp. 153-160.

[18] R. Al-Jarrah and H. Roth, "Blimp based on embedded computer vision and fuzzy control for following ground vehicles," in *Proc. the 3rd IFAC Symposium on Telematics Applications, The International Federation of Automatic Control*, Yonsei University, Seoul, Korea, November 2013, pp. 7-12.

[19] R. Al-Jarran and H. Roth, "Design blimp robot based on embedded system and software architecture with high level communication and fuzzy logic," in *Proc. the 9th International Symposium on Mechatronis and its Applications (ISMA13)*, Amman, Jordan, April 2013.

[20] H. Bay, A. Ess, T. Tuyelaars, and V. Gool," Speeded up robust features," in *Proc. European Conference on Computer Vision*, 2006, pp. 404-417.

[21] M. Fischer and R. C. Bolles, "Random sample consensus: a paradigm for model fitting with applications to image analysis and automated cartography," *Communication of the ACM*, vol. 24, no. 6, pp. 381-395, 1981.

[22] J. Cliff, "Measurement of possibilistic histograms from interval data," *General Systems*, vol. 26, issue1-2, pp. 09-33, 1997.

Rami Al-Jarrah was born in Jordan in 1979 who completed his MSc degree in mechatronics engineering at Jordan University of Science and Technology JUST, Jordan in 2004. He is currently a PhD candidate and research assistant at Control and Automatic Engineering Department (RST), Faculty of Electrical Engineering and Informatics, Siegen University, Germany. His research interests are fuzzy logic analysis, image processing and computer vision, wireless sensor networks as well as aerial robots navigation. He awarded the best excellent paper in ICCAE 2013. He worked as a lecturer in Mechanical Engineering Department at JUST 2005 as well as at the Computer Engineering Department at Vocational Training Corporation, Saudi Arabia, 2006-2009.

Hubert Roth was born in Oppenau, Germany in 1954 who completed a doctorate degree at Karlsruhe Technical University, Germany in 1983. He employed at Dornier System GmbH in Friedrichshafen, Aerospace Systems Department 1983-1988. Currently he is the chair in Control and Automatic Engineering Department (RST) a Siegen University, Faculty of Electrical Engineering and Informatics since 2001.

Prof. Dr.-Ing. Roth is a vice director of "Technical Committee on Computers and Telematics" of International Federation of Automatic Control (IFAC) since 2008 and vice director of Centre for International Capacity Development (CICD) since 2009.